Inorganic Chemistry

Photochemical Synthesis and Reactivity Studies of Dirhenacarboranes

Michael J. Carr, Thomas D. McGrath, and F. Gordon A. Stone*

Department of Chemistry and Biochemistry, Baylor University, Waco, Texas 76798-7348

Ultraviolet irradiation of [PPh$_4$][*closo*-1-CB$_8$H$_9$] with [Re$_2$(CO)$_{10}$] in THF (tetrahydrofuran) at ambient temperature affords the dirhenacarborane anion [6,10-{Re(CO)$_4$}-10-(μ-H)-6,6,6-(CO)$_3$-*closo*-6,1-ReCB$_8$H$_8$]$^-$, isolated as its [PPh$_4$]$^+$ salt (**1**). Further irradiation of **1** yields a second isomeric anion [6,10-{Re(CO)$_4$}-6-(μ-H)-10,10,10-(CO)$_3$-*closo*-10,1-ReCB$_8$H$_8$]$^-$ that was characterized as a [N(PPh$_3$)$_2$]$^+$ salt (**2**). Reaction of **1** with NOBF$_4$ produces the neutral dirhenacarborane compound [8,10-{Re(CO)$_4$}-8,10-(μ-H)$_2$-6,6-(CO)$_2$-6-NO-*closo*-6,1-ReCB$_8$H$_7$] (**3**). Compounds **1**–**3** all consist of a central {*closo*-ReCB$_8$} cluster with a second rhenium center which is exo-polyhedral. Attempts to substitute the carbonyl ligands of **3** with other donor ligands such as phosphines, isocyanides, or alkynes resulted in loss of the exo-polyhedral rhenium moiety and formation of a monorhenium anion, [6,6-(CO)$_2$-6-NO-*closo*-6,1-ReCB$_8$H$_9$]$^-$, isolated as its [N(PPh$_3$)$_2$]$^+$ salt (**4**). The heterometallic dimetallacarborane species, [6,7,10-{Cu(PPh$_3$)}-7,10-(μ-H)$_2$-6,6-(CO)$_2$-6-NO-*closo*-6,1-ReCB$_8$H$_7$] (**5**) and [6,7-{Au(PPh$_3$)}-7-(μ-H)-6,6-(CO)$_2$-6-NO-*closo*-6,1-ReCB$_8$H$_8$] (**6**) were formed from reactions of **4** with {Cu(PPh$_3$)}$^+$ and {Au(PPh$_3$)}$^+$, respectively. Similarly, reaction of **4** with {Ir(CO)(PPh$_3$)$_2$}$^+$ afforded two products, [6,10-{Ir(μ-PPh$_2$)(Ph)(CO)(PPh$_3$)}-10-(μ-H)-6-CO-6-NO-*closo*-6,1-ReCB$_8$H$_8$] (**7**) and [6,9,10-{Ir(μ-PPh$_2$)(H)(PPh$_3$)}-9-(μ-H)-6-CO-6-NO-10-Ph-*closo*-6,1-ReCB$_8$H$_8$] (**8**). The solid-state structures of compounds **1**–**8** were all unequivocally established by single-crystal X-ray diffraction experiments.

Introduction

The discovery of the "Brellochs reaction"[1] has allowed us to extend our research upon metal–monocarbollide complexes, which was previously limited to icosahedral {MCB$_{10}$} clusters,[2,3] to studies of smaller, sub-icosahedral species. This breakthrough provided a facile route to *nido*- and *arachno*-{CB$_9$} species from commercially available decaborane (B$_{10}$H$_{14}$). When treated with suitable metal carbonyl precursors these 10-vertex monocarborane clusters afford 11- and 12-vertex {*closo*-M$_n$CB$_9$} clusters (M = Re,[4] Mn,[5] Mo,[6] *n* = 1; M = Co,[7] *n* = 2). Monocarboranes with

fewer than 10 vertexes can be synthesized via further manipulation of the initial *nido*- and *arachno*-{CB$_9$} monocarboranes.[8] Of particular interest here is the behavior of the anions [*closo*-CB$_n$H$_{n+1}$]$^-$ (*n* = 6, 7, 8) in reactions with metal carbonyls, as related larger carborane molecules undergo oxidative insertion reactions with M^0 fragments to form metallacarboranes.[9] This methodology has led to the successful synthesis of sub-icosahedral metallacarboranes that contain Mn, Re, Fe, Ru, Co, and Ir moieties.[7,10–12] Many of the resulting small metallacarborane products remain anions

* To whom correspondence should be addressed. E-mail: gordon_stone@baylor.edu.

(1) Brellochs, B. In *Contemporary Boron Chemistry*; Davidson, M. G., Hughes, A. K., Marder, T. B., Wade, K., Eds.; Royal Society of Chemistry: Cambridge, U.K., 2000; p 212.
(2) McGrath, T. D.; Stone, F. G. A. *J. Organomet. Chem.* **2004**, *689*, 3891.
(3) McGrath, T. D.; Stone, F. G. A. *Adv. Organomet. Chem.* **2005**, *53*, 1.
(4) Du, S.; Kautz, J. A.; McGrath, T. D.; Stone, F. G. A. *Organometallics* **2003**, *22*, 2842.
(5) (a) Du, S.; Farley, R. D.; Harvey, J. N.; Jeffery, J. C.; Kautz, J. A.; Maher, J. P.; McGrath, T. D.; Murphy, D. M.; Riis-Johannessen, T.; Stone, F. G. A. *Chem. Commun.* **2003**, 1846. (b) Du, S.; Jeffery, J. C.; Kautz, J. A.; Lu, X. L.; McGrath, T. D.; Miller, T. A.; Riis-Johannessen, T.; Stone, F. G. A. *Inorg. Chem.* **2005**, *44*, 2815.
(6) Lei, P.; McGrath, T. D.; Stone, F. G. A. *Chem. Commun.* **2005**, 3706.

(7) Lu, X. L.; McGrath, T. D.; Stone, F. G. A. *Organometallics* **2006**, *25*, 2590.
(8) (a) Brellochs, B.; Backovsky, J.; Štíbr, B.; Jelínek, T.; Holub, J.; Bakardjiev, M.; Hnyk, D.; Hofmann, M.; Císařová, I.; Wrackmeyer, B. *Eur. J. Inorg. Chem.* **2004**, *3605*. (b) Štíbr, B. *Pure Appl. Chem.* **2003**, *75*, 1295. (c) Franken, A.; Jelínek, T.; Taylor, R. G.; Ormsby, D. L.; Kilner, C. A.; Clegg, W.; Kennedy, J. D. *Dalton Trans.* **2006**, 5753.
(9) For example: (a) Green, M.; Howard, J. A. K.; Spencer, J. L.; Stone, F. G. A. *J. Chem. Soc., Chem. Commun.* **1974**, 153. (b) Barker, G. K.; Green, M.; Stone, F. G. A.; Welch, A. J.; Wolsey, W. C. *J. Chem. Soc., Chem. Commun.* **1980**, 627.
(10) Franken, A.; McGrath, T. D.; Stone, F. G. A. *Organometallics* **2005**, *24*, 5157.
(11) Franken, A.; McGrath, T. D.; Stone, F. G. A. *Inorg. Chem.* **2006**, *45*, 2669.
(12) Franken, A.; Lei, P.; McGrath, T. D.; Stone, F. G. A. *Chem. Commun.* **2006**, 3423.

Chart 1
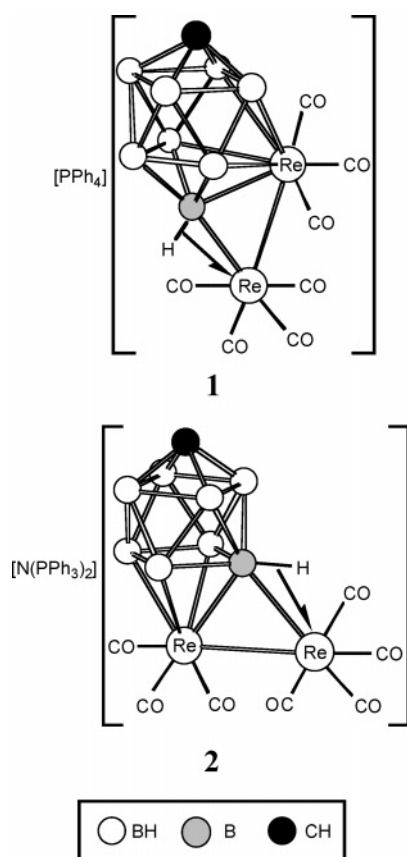
and are therefore susceptible to further reaction with transition metal cations thus providing a ready route to heterometallic species.[7,10,11,13]

In extension of this research into sub-icosahedral metallacarborane we herein present the synthesis of dirhenacarborane species {Re₂CB₈} formed initially via oxidative insertion of $[Re_2(CO)_{10}]$ into $[closo\text{-}1\text{-}CB_8H_9]^-$ using photochemical methods. Heterometallic monocarborane complexes {MReCB₈} (M = Cu, Au, and Ir) formed by addition of transition metal cations to a monorhenium {ReCB₈} substrate are also described.

Results and Discussion

Photochemical Route to Dirhenacarborane Isomers. The dirhenacarborane anion $[6,10\text{-}\{Re(CO)_4\}\text{-}10\text{-}(\mu\text{-}H)\text{-}6,6,6\text{-}(CO)_3\text{-}closo\text{-}6,1\text{-}ReCB_8H_8]^-$ was obtained by the photochemical reaction of $[PPh_4][closo\text{-}1\text{-}CB_8H_9]$ with $[Re_2(CO)_{10}]$ in THF at ambient temperature for 2 h and isolated as the $[PPh_4]^+$ salt **1** (Chart 1). An isomer of this anion can be obtained when **1** is irradiated for a further 3 h, again at ambient temperature in THF. Metathesis by the addition of $[N(PPh_3)_2]Cl$ allowed the isolation of $[6,10\text{-}\{Re(CO)_4\}\text{-}6\text{-}(\mu\text{-}H)\text{-}10,10,10\text{-}(CO)_3\text{-}closo\text{-}10,1\text{-}ReCB_8H_8]^-$ as its $[N(PPh_3)_2]^+$ salt (**2**). There are few reported examples of using photochemical methods for the synthesis of metallacarbo-

(13) (a) McGrath, T. D.; Du, S.; Hodson, B. E.; Lu, X. L.; Stone, F. G. A. *Organometallics* **2006**, *25*, 4444. (b) McGrath, T. D.; Du, S.; Hodson, B. E.; Stone, F. G. A. *Organometallics* **2006**, *25*, 4452.

ranes from metal carbonyls.[12,14] In those reactions, the incorporation of the metal center is accompanied by the insertion of a carbonyl group into the cluster, giving products that contain two additional cage vertexes, one metal center, and one carbon atom, thus differing from the metal-only insertion reported here. Attempts to produce **1** and **2** by the more conventional thermal route proved unsuccessful, as did the synthesis of analogous manganese complexes, where both thermal and photochemical routes failed.

Physical and spectroscopic data for compounds **1** and **2** are presented in Tables 1 and 2, and their solid-state structures were established by X-ray diffraction studies. The anions of the two complexes are shown in Figures 1 and 2, respectively, and are seen in each case to consist of a central $closo$-10-vertex {ReCB₈} cluster with the second rhenium center bonded exo-polyhedrally to the cage. The two isomers differ in the location of their cluster rhenium vertexes. In the anion of **1**, the rhenium center is in the 6-position, ligated by five cage boron atoms, whereas in **2** the cluster rhenium atom is unusually in the apical 10-position and bonded to only four cage boron atoms. The exo-polyhedral unit in each case is attached to the polyhedron by a Re−Re bond [Re(6)−Re(61) = 2.9953(2) Å in **1**; Re(10)−Re(61) = 2.9600(6) Å in **2**] and a B−H⌐Re agostic-type interaction [B(10)−Re(61) = 2.309(3) Å in **1**; B(6)···Re(61) = 2.400(7) Å in **2**]. The Re−Re bond in both compounds can be viewed as supplying the extra electron to give the required 11 skeletal electron pair count for conventional closo 10-vertex species. In the anions of both **1** and **2**, the rhenium centers are formally in the +1 oxidation state and possess pseudo-octahedral coordination spheres where the cage rhenium atoms are also bonded to three carbonyl groups and the exo-polyhedral rhenium centers are bonded to four carbonyl ligands.

The IR spectrum of **1** shows five strong CO stretching bands between 2095 and 1910 cm⁻¹, while its ¹¹B{¹H} NMR spectrum contains a 1:3(1 + 2 coincidence):2:2 set of resonances, consistent with molecular mirror symmetry. The highest frequency signal, at δ 81.7, may be assigned to the $B(10)$−Re nucleus, as similar four-coordinate boron nuclei in 10-vertex systems are usually relatively deshielded.[15] Furthermore, proton coupling, which is smaller for B−H−M protons, is unresolved for this resonance in the ¹H-coupled ¹¹B NMR spectrum, whereas the other signals clearly become doublets due to their associated terminal hydrogen atoms. Five resonances in the ¹³C{¹H} NMR spectrum, between δ 195.5 and 187.3, can be assigned to the carbonyl groups, and a broad resonance at δ 63.3 is assigned to the cage carbon atom. In the ¹H NMR spectrum a diagnostic broad quartet resonance of unit integral is seen at δ −5.84 [J(BH) = 64 Hz] and is assigned to the B−H⌐Re linkage.[15]

For compound **2** the IR spectrum similarly shows five strong bands in the CO region between 2090 and 1885 cm⁻¹.

(14) (a) Wegner, P. A.; Guggenberger, L. J.; Muetterties, E. L. *J. Am. Chem. Soc.* **1970**, *92*, 3473. (b) Schultz, R. V.; Sato, F.; Todd, L. J. *J. Organomet. Chem.* **1977**, *125*, 115. (c) Fontaine, X. L. R.; Greenwood, N. N.; Kennedy, J. D.; MacKinnon, P. I.; Macpherson, I. *J. Chem. Soc., Dalton Trans.* **1987**, 2385.

(15) Brew, S. A.; Stone, F. G. A. *Adv. Organomet. Chem.* **1993**, *35*, 135.

Table 1. Analytical and Physical Data[a]

compd		color	$\nu_{max}(CO)^a/cm^{-1}$	anal./% [b]		
				C	H	N
1	[PPh$_4$][6,10-{Re(CO)$_4$}-10-(μ-H)-6,6,6-(CO)$_3$-*closo*-6,1-ReCB$_8$H$_8$]	orange	2095 s, 2002 vs, 1948 s, 1931 s, 1910 s	37.9 (37.9)	2.8 (2.9)	
2	[N(PPh$_3$)$_2$][6,10-{Re(CO)$_4$}-6-(μ-H)-10,10,10-(CO)$_3$-*closo*-10,1-ReCB$_8$H$_8$]	yellow	2090 m, 1995 vs, 1937 s, 1913 s, 1885 m	43.8 (43.5)	3.2 (3.2)	1.2 (1.2)
3	[8,10-{Re(CO)$_4$}-8,10-(μ-H)$_2$-6,6-(CO)$_2$-6-NO-*closo*-6,1-ReCB$_8$H$_7$]	yellow	2129 m, 2072 s, 2033 vs, 1992 s	12.6 (12.4)	1.4 (1.3)	2.1 (2.1)
4	[N(PPh$_3$)$_2$][6,6-(CO)$_2$-6-NO-*closo*-6,1-ReCB$_8$H$_9$]	orange	2032 s, 1972 s	50.9 (51.0)	4.3 (4.3)	3.1 (3.1)
5	[6,7,10-{Cu(PPh$_3$)}-7,10-(μ-H)$_2$-6,6-(CO)$_2$-6-NO-*closo*-6,1-ReCB$_8$H$_7$]	yellow	2059 s, 2007 s	35.9 (35.7)	3.4 (3.4)	2.1 (2.0)
6	[6,7-{Au(PPh$_3$)}-7-(μ-H)-6,6-(CO)$_2$-6-NO-*closo*-6,1-ReCB$_8$H$_8$]	yellow	2059 s, 2007 s	29.3 (29.4)[c]	2.9 (2.9)	1.6 (1.6)
7	[6,10-{Ir(μ-PPh$_2$)(Ph)(CO)(PPh$_3$)}-10-(μ-H)-6-CO-6-NO-*closo*-6,1-ReCB$_8$H$_8$]	yellow	2060 s, 2033 s	40.1 (40.6)[d]	3.7 (3.5)	1.2 (1.3)
8	[6,9,10-{Ir(μ-PPh$_2$)(H)(PPh$_3$)}-9-(μ-H)-6-CO-6-NO-10-Ph-*closo*-6,1-ReCB$_8$H$_8$]	red	2002 s	41.8 (41.6)[c]	3.7 (3.6)	1.3 (1.3)

[a] Measured in CH$_2$Cl$_2$; a broad, medium-intensity band observed at ca. 2500−2550 cm^{-1} in the spectra of all compounds is due to B−H absorptions. In addition, ν_{max}(NO)/cm^{-1}: for **3**, 1747 s; for **4**, 1698 s; for **5**, 1736 s; for **6**, 1742 s; for **7**, 1719 s; and for **8**, 1698 s. [b] Calculated values are given in parentheses. [c] Solid contains 0.5 mol equiv of CH$_2$Cl$_2$. [d] Solid contains 1.0 mol equiv of CH$_2$Cl$_2$.

Table 2. ^{1}H, ^{13}C, ^{11}B, and ^{31}P NMR Data[a]

compd	^{1}H/δ^b	^{13}C/δ^c	^{11}B/δ^d	^{31}P/δ^e
1	7.90−7.59 (m, 20H, Ph), 4.17 (br s, 1H, cage CH), −5.84 [br q, J(BH) = 64, 1H, B−H⇀Re]	195.5, 195.0, 191.2, 190.7, 187.3 (CO), 136.1−117.4 (Ph), 63.3 (br, cage C)	81.7 [B(10)], −4.2 (3B), −18.8 (2B), −20.1 (2B)	23.4
2	7.92−7.56 (m, 30H, Ph), 3.67 (br s, 1H, cage CH), −11.20 [br q, J(BH) = 68, 1H, B−H⇀Re]	202.5, 195.2, 191.2 (CO), 136.2−117.4 (Ph), 94.7 (br, cage C)	22.1 [B(6)], −4.2 (4B), −9.1 (2B), −17.3	21.2
3	6.17 (br s, 1H, cage CH), −1.51 [br q, J(BH) = 91, 1H, B−H⇀Re], −5.71 [br q, J(BH) = 71, 1H, B−H⇀Re]	192.7, 185.0, 184.0, 180.8 (CO), 67.7 (br, cage C)	28.0, −5.2 (2B), −15.2 (3B), −22.8 (2B)	
4	7.68−7.46 (m, 30H, Ph), 5.48 (br s, 1H, cage CH)	200.6 (CO), 134.0−126.8 (Ph), 59.1 (br, cage C)	48.2, −8.1, −9.2 (2B), −23.3 (2B), −27.7 (2B)	21.2
5	7.72−7.42 (m, 15H, Ph), 6.12 (br s, 1H, cage CH)	192.7 (CO), 134.2−129.7 (Ph), 69.0 (br, cage C)	32.5, −9.0 (3B), −21.1 (2B), −28.7 (2B)	9.9 (br)
6	7.61−7.55 (m, 15H, Ph), 5.91 (br s, 1H, cage CH)	191.4 (CO), 134.4−129.1 (Ph), 66.3 (br, cage C)	38.5, −10.9, −11.7 (2B), −20.3 (2B), −27.0 (2B)	40.7
7[f]	7.48−7.43 (m, 30H, Ph), 5.80 (br s, 1H, cage CH), −4.97 (br, 1H, B−H⇀Ir)		62.9 [B(10)], −7.3 (br, 2B), −10.4, −16.0 (br, 3B), −20.0	106.9 {Ir−(PPh$_2$)−Re}, 17.2 {Ir(PPh$_3$)}
8	7.43−6.93 (m, 30H, Ph), 5.80 (br s, 1H, cage CH), −4.68 (br, 1H, B−H⇀Ir), −18.26 (br, 1H, Ir−H)	194.8 (CO), 134.6−126.9 (Ph), 63.4 (br, cage C)	54.8 [B(10)], −2.7, −4.8, −14.9 (2B), −17.7, −29.3, −36.6	112.9 {Ir−(PPh$_2$)−Re}, 26.7 {Ir(PPh$_3$)}

[a] Chemical shifts (δ) in ppm, coupling constants (J) in Hz, measurements at ambient temperatures in CD$_2$Cl$_2$. [b] Resonances for terminal BH protons occur as broad unresolved signals in the range δ ca. −1 to +4. [c] ^{1}H-decoupled chemical shifts are positive to high frequency of SiMe$_4$. [d] ^{1}H-decoupled chemical shifts are positive to high frequency of BF$_3$·Et$_2$O (external); resonances have singlet multiplicity and are of unit integral, except where indicated. [e] ^{1}H-decoupled chemical shifts are positive to high frequency of 85% H$_3$PO$_4$ (external). [f] No satisfactory ^{13}C{^{1}H} NMR spectrum could be obtained for **7** due to its instability in solution.

Its ^{11}B{^{1}H} NMR spectrum shows four resonances of relative intensity 1:4(2 + 2 coincidence):2:1, again consistent with the solid-state structure. The lowest field resonance, δ 22.1, again can be assigned to the B−H⇀Re nucleus on the basis of a relatively small proton coupling in the ^{11}B NMR spectrum. The ^{13}C{^{1}H} NMR spectrum of **2** shows just three resonances (δ 202.5, 192.5, and 191.2) for the five chemically different carbonyls, indicating that some signals are coincident. A broad resonance at δ 94.7 that can be assigned to the cage carbon atom is at a notably higher frequency than the corresponding signal for compound **1**. As with compound **1**, the ^{1}H NMR spectrum of compound **2** shows a diagnostic broad quartet resonance, δ −11.20 [J(BH) = 68 Hz], that is assigned to the single B−H⇀Re linkage. This

resonance is at significantly higher field than in compound **1**, indicating that more electron density is associated with the B−H⇀Re linkage in compound **2**.

Although it was possible to separate and fully characterize both dirhenacarborane isomers, the yield of compound **2** (26%) was unfavorable. It is hypothesized that when compound **1** is subjected to further photochemical irradiation, monorhenium byproducts may also form via loss of the exopolyhedral rhenium atom. The requirement of preparative thin-layer chromatography for the isolation of pure compound **2** (due to the inherent similarities of the two compounds) also contributes to its low yield. For these reasons the derivative chemistry described below is based on the first, more easily obtained isomer **1**.
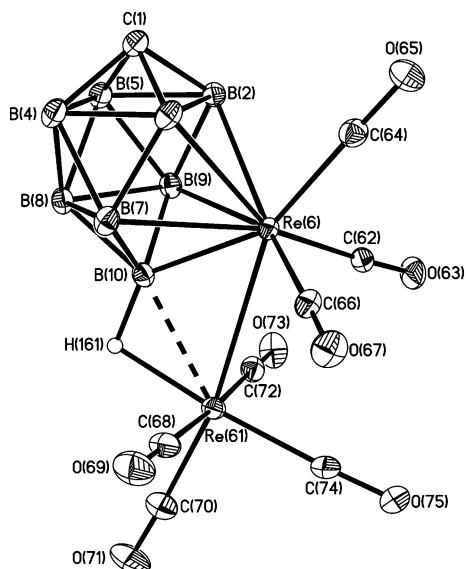
Figure 1. Structure of the anion of **1** showing the crystallographic labeling scheme. Selected distances (Å) are Re(6)−Re(61) 2.9953(2), Re(6)−B(2) 2.390(3), Re(6)−B(3) 2.378(3), Re(6)−B(7) 2.445(3), Re(6)−B(9) 2.450(3), Re(6)−B(10) 2.168(3), Re(6)−C(62) 1.942(3), Re(6)−C(64) 1.948(3), Re(6)−C(66) 1.939(3), C(62)−O(63) 1.147(3), C(64)−O(65) 1.146(3), C(66)−O(67) 1.154(3), Re(61)···B(10) 2.309(3), Re(61)−C(68) 2.003(3), Re(61)−C(70) 1.930(3), Re(61)−C(72) 2.001(3), Re(61)−C(74) 1.943(3), C(68)−O(69) 1.131(3), C(70)−O(71) 1.143(3), C(72)−O(73) 1.133(3), C(74)−O(75) 1.148(3). Average cage B−B and C−B distances are 1.808(4) and 1.609(4) Å, respectively. In this and subsequent figures, thermal ellipsoids are drawn with 40% probability and, for clarity, only chemically significant hydrogen atoms are shown.
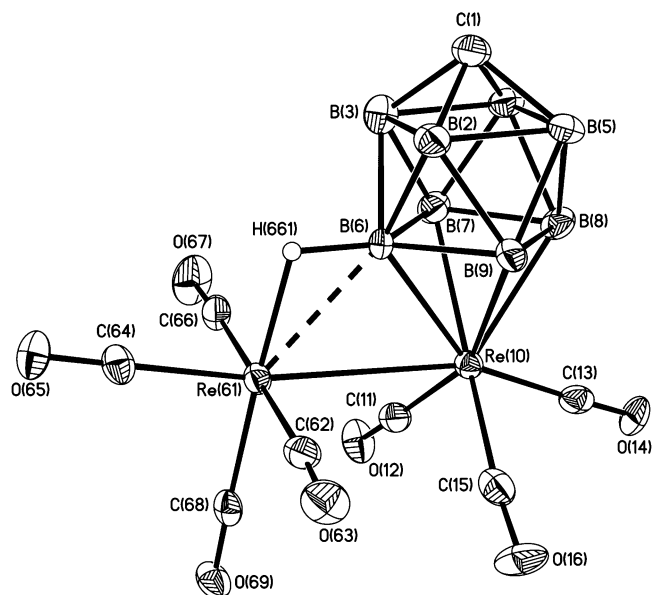
Figure 2. Structure of the anion of **2** showing the crystallographic labeling scheme. Selected distances (Å) are Re(10)−Re(61) 2.9600(6), Re(10)−B(6) 2.231(7), Re(10)−B(7) 2.308(7), Re(10)−B(8) 2.261(7), Re(10)−B(9) 2.316(7), Re(10)−C(11) 1.959(8), Re(10)−C(13) 1.951(7), Re(10)−C(15) 1.944(8), C(11)−O(12) 1.150(7), C(13)−O(14) 1.153(7), C(15)−O(16) 1.151(8), Re(61)···B(6) 2.400(7), Re(61)−C(62) 1.992(7), Re(61)−C(64) 1.940(7), Re(61)−C(66) 2.024(8), Re(61)−C(68) 1.954(7), C(62)−O(63) 1.137(7), C(64)−O(65) 1.138(7), C(66)−O(67) 1.127(8), C(68)−O(69) 1.140(7). Average cage B−B and C−B distances are 1.824(10) and 1.595(10) Å, respectively.

Formation of Additional Dirhenium and Monorhenium Species. Preliminary reactivity studies showed that compound **1** is resistant to the substitution of its CO ligands by

Chart 2
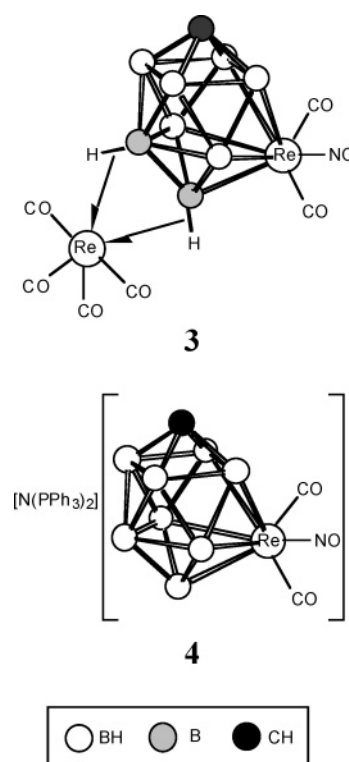
other donor molecules such as phosphines, isocyanides, and alkynes. In efforts to promote the replacement of the carbonyl ligands the use of Me₃NO, elevated reaction temperatures and photochemical irradiation were all employed but all proved unsuccessful. As compound **1** is anionic, these observations were not surprising as similar anionic complexes have also proved resistant to these types of reactions.[3] The monoanionic nature of compound **1** suggested that neutral trimetallic complexes could feasibly be formed by the addition of another cationic transition metal fragment. However, attempts to treat **1** with{Cu(PPh₃)}⁺ and {Au-(PPh₃)}⁺ were unfruitful. It is notable that the analogous 11-vertex dirhenacarborane anion [1,3,6-{Re(CO)₃}-3,6-(μ-H)₂-1,1,1-(CO)₃-2-Ph-*closo*-1,2-ReCB₉H₇]⁻ also failed to react with {Cu(PPh₃)}⁺ and {Au(PPh₃)}⁺ cations.[4] Nevertheless, an attempt to replace a CO group by [NO]⁺ using NOBF₄, and hence form a neutral species, was successful.

Addition of NOBF₄ to a solution of compound **1** in CH₂-Cl₂ resulted in the formation of the neutral dirhenacarborane species [8,10-{Re(CO)₄}-8,10-(μ-H)₂-6,6-(CO)₂-6-NO-*closo*-6,1-ReCB₈H₇] (**3**) (Chart 2). The solid-state structure of **3** as determined by an X-ray diffraction study is illustrated in Figure 3. The expected exchange of a CO ligand for the [NO]⁺ species is allied with the more unexpected cleavage of the Re−Re bond. The [NO]⁺ species substitutes a CO ligand on the cage rhenium vertex and the exo-polyhedral rhenium center migrates, relative to its site in **1**, and is now attached to the closo 10-vertex cage via two B−H→Re linkages [B(8)−Re(81) = 2.436(6) Å and B(10)−Re(81) = 2.463(5) Å]. Physical and spectroscopic details for compound **3** are shown in Tables 1 and 2. The IR spectrum shows four CO bands between 2130 and 1992 cm⁻¹, as well as a band at 1747 cm⁻¹ assigned to the NO ligand. The ¹¹B{¹H} NMR
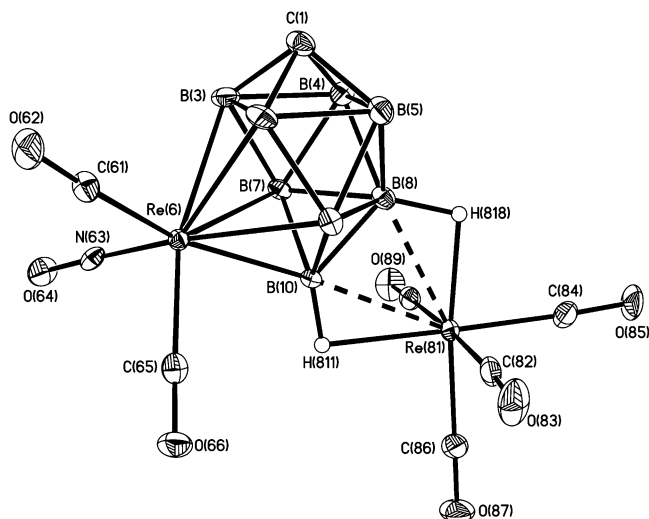
Figure 3. Structure of compound **3** showing the crystallographic labeling scheme. Two crystallographically independent molecules are present in the asymmetric unit, of which one is shown here. Selected distances (Å) are Re(6)−B(2) 2.402(6), Re(6)−B(3) 2.385(6), Re(6)−B(7) 2.368(5), Re(6)−B(9) 2.406(6), Re(6)−B(10) 2.167(5), Re(6)−C(61) 1.991(5), Re(6)−C(65) 1.994(6), Re(6)−N(63) 1.813(5), C(61)−O(62) 1.132(7), C(65)−O(66) 1.124(7), N(63)−O(64) 1.168(6), Re(81)···B(8) 2.436(6), Re(81)···B(10) 2.463(5), Re(81)−C(82) 2.006(6), Re(81)−C(84) 1.934(5), Re(81)−C(86) 1.946(6), Re(81)−C(88) 2.013(6), C(82)−O(83) 1.137(6), C(84)−O(85) 1.140(7), C(86)−O(87) 1.139(7), C(88)−O(89) 1.132(7). Average cage B−B and C−B distances are 1.808(9) and 1.598(9) Å, respectively.

spectrum shows four peaks of relative intensity 1:2:3(1 + 2 coincidence):2, and the ^{13}C{^{1}H} NMR spectrum shows four resonances between δ 192.7 and 180.8, indicating four chemically different CO groups, as well as a broad resonance at δ 67.7 corresponding to the cage carbon nucleus. All of this is consistent with the symmetry seen in the solid state. In the ^{1}H NMR spectrum, two characteristic broad quartet resonances are observed at δ −1.51 [*J*(BH) = 91 Hz] and −5.71 [*J*(BH) = 71 Hz] and are assigned to the two B−H⇀Re linkages.

As compound **3** is uncharged, it was intuitive to attempt the ligand substitution reactions that were not successful for anionic compound **1**. However, all efforts to substitute the carbonyl ligands of compound **3** with other donors such as phosphines, isocyanides, and alkynes resulted in the formation of a single rhenacarborane anion that could be isolated after addition of [N(PPh$_3$)$_2$]Cl and identified as [N(PPh$_3$)$_2$]-[6,6-(CO)$_2$-6-NO-*closo*-6,1-ReCB$_8$H$_9$] (**4**). Presumably, the added ligands react preferentially with the exo-polyhedral rhenium center cleaving it from the cluster and forming {Re-(CO)$_4$L$_2$}$^+$-type species, although no attempt was made to isolate the latter. Physical and spectroscopic data for compound **4** are presented in Tables 1 and 2, and the solid-state structure of the anion of **4**, as characterized by an X-ray diffraction study, is shown in Figure 4. In compounds **3** and **4** the stepwise migration of the exo-polyhedral rhenium center is observed, first with the cleavage of the Re−Re bond in compound **3** and, ultimately, with the formation of the monorhenium anion of **4**. Two strong CO absorption bands (2032 and 1972 cm^{-1}) appear in the IR spectrum of **4**, as does a single NO absorption band at 1698 cm^{-1}. The ^{11}B-{^{1}H} NMR spectrum of compound **4** is consistent with the inherent symmetry of the solid-state structure and displays
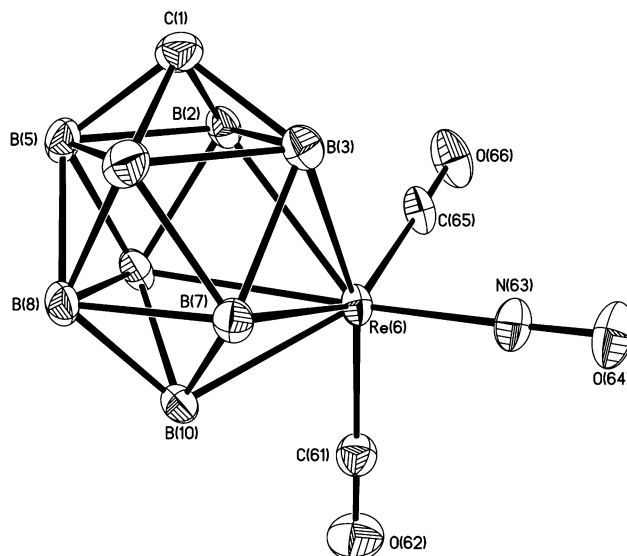
Figure 4. Structure of the anion of **4** showing the crystallographic labeling scheme. Selected distances (Å) are Re(6)−B(2) 2.364(3), Re(6)−B(3) 2.361(3), Re(6)−B(7) 2.390(3), Re(6)−B(9) 2.416(3), Re(6)−B(10) 2.203(3), Re(6)−C(61) 1.951(3), Re(6)−C(65) 1.946(3), Re(6)−N(63) 1.843(2), C(61)−O(62) 1.146(3), C(65)−O(66) 1.146(3), N(63)−O(64) 1.167(3). Average cage B−B and C−B distances are 1.812(4) and 1.601(4) Å, respectively.

a 1:1:2:2:2 set of resonances, all of which are similarly coupled to terminal B−H nuclei in the proton coupled ^{11}B NMR spectrum. The ^{13}C{^{1}H} NMR spectrum shows just one peak at δ 200.6 for the two CO ligands plus a broad resonance (δ 59.1) that corresponds to the cage carbon nucleus.

Synthesis of Heterometallic Dimetallacarborane Species. Given the anionic nature of compound **4**, it was decided to investigate its reactivity with cationic transition metal fragments in the hope of forming neutral heterometallic dimetallacarborane species. Related 11- and 12-vertex, *closo*-monorhenacarborane compounds have been reported that were synthesized directly from {CB$_9$} and {CB$_{10}$} moieties.[4,16] These differ from compound **4**, however, in that they are dianionic, as their rhenium centers bear three carbonyl ligands compared to two carbonyls and a nitrosyl ligand in **4**. Reactions of those dianions, [1,1,1-(CO)$_3$-2-Ph-*closo*-1,2-ReCB$_9$H$_9$]$^{2-}$ and [2,2,2-(CO)$_3$-*closo*-2,1-ReCB$_{10}$H$_{11}$]$^{2-}$, with various cationic transition metal fragments to form heterometallic metallacarborane species have proved particularly successful.[4,13a,16,17]

Compound **4** did indeed react with the transition metal fragments {Cu(PPh$_3$)}$^+$ and {Au(PPh$_3$)}$^+$, which were formed in situ from [CuCl(PPh$_3$)]$_4$/TlPF$_6$ or [AuCl(PPh$_3$)]/TlPF$_6$ mixtures, respectively, to yield the bimetallic species [6,7,10-{Cu(PPh$_3$)}-7,10-(µ-H)$_2$-6,6-(CO)$_2$-6-NO-*closo*-6,1-ReCB$_8$H$_7$] (**5**) and [6,7-{Au(PPh$_3$)}-7-(µ-H)-6,6-(CO)$_2$-6-NO-*closo*-6,1-ReCB$_8$H$_8$] (**6**) (see Chart 3). Compounds **5** and **6** were characterized by X-ray diffraction studies, and their solid-state structures were found to be very similar: the only

(16) Blandford, I.; Jeffery, J. C.; Jelliss, P. A.; Stone, F. G. A. *Organometallics* **1998**, *17*, 1402.

(17) Jeffery, J. C.; Jelliss, P. A.; Rees, L. H.; Stone, F. G. A. *Organometallics* **1998**, *17*, 2258.

Chart 3

5

6

| ○ BH | ◐ B | ● CH |
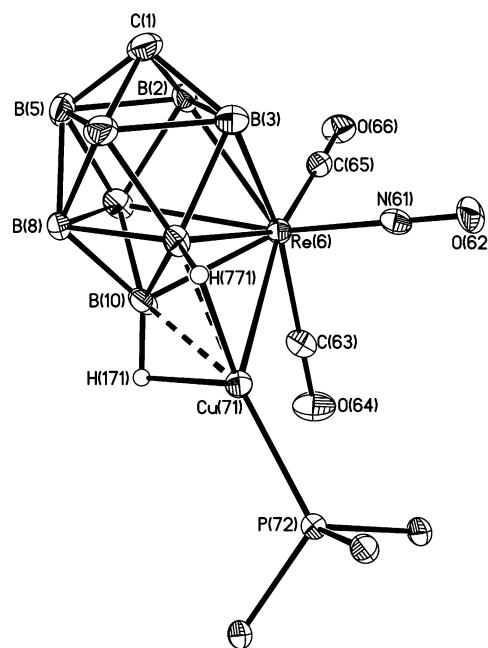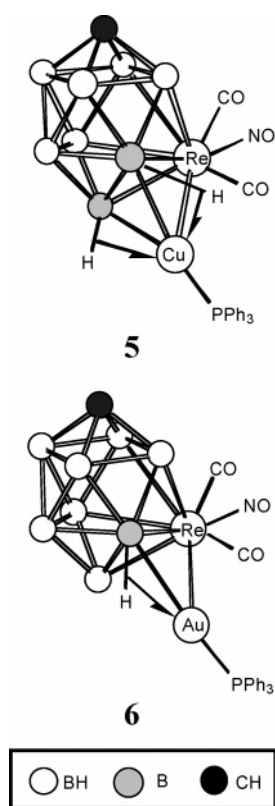
Figure 5. Structure of compound **5** showing the crystallographic labeling scheme. Only the ipso carbon atoms of the phosphine phenyl rings are shown for clarity. Selected distances (Å) are Re(6)−Cu(71) 2.8240(8), Re(6)−B(2) 2.347(6), Re(6)−B(3) 2.372(7), Re(6)−B(7) 2.428(6), Re(6)−B(9) 2.412(6), Re(6)−B(10) 2.236(7), Re(6)−C(63) 1.935(6), Re(6)−C(65) 1.978(6), Re(6)−N(61) 1.843(5), C(63)−O(64) 1.151(7), C(65)−O(66) 1.121(7), N(61)−O(62) 1.177(6), Cu(71)−P(72) 2.1858(15), Cu(71)···B(7) 2.117(7), Re(71)···B(10) 2.183(6). Average cage B−B and C−B distances are 1.807(10) and 1.612(9) Å, respectively.

significant difference is that in compound **6** the {Au(PPh₃)}⁺ is linked to the cluster via a single B−H⇀M interaction whereas compound **5** contains two such linkages. The Cu−Re interatomic distance is 2.8240(8) Å in **5** and the Au−Re interatomic distance is 3.0081(6) Å in **6**; both distances are as expected for such metal−metal interactions. Figure 5 shows the molecular structure of compound **5**, which merits little further comment.

The IR spectrum for compound **5** shows two bands for CO ligands (2059 and 2007 cm⁻¹) and a single absorption at 1736 cm⁻¹ corresponding to the NO ligand. The ¹¹B{¹H} NMR for compound **5** is similar to that of compound **4** and shows a 1:3(1 + 2 coincidence):2:2 set of resonances with chemical shifts similar to those observed for **4**. This suggests that the exo-polyhedral copper fragment is fluxional with respect to the cluster surface, as has been observed previously in similar {Cu(PPh₃)}⁺ derivatives of metallacarborane anions.[7,10,11] Such processes are very fast on the NMR time scale even at low temperatures,[17,18] meaning that no signals for the protons involved in the B−H⇀Cu bridges are observed in the ¹H NMR spectrum of **5**, as is typical. Investigations of similar dynamic processes in cupracarboranes have used low-temperature NMR studies to speculate on such processes without unequivocally revealing their exact nature.[19] Further studies of these dynamic processes in **5** would require extensive investigations and comparisons with

similar species that are beyond the scope of this paper. A single peak at δ 192.7 in the ¹³C{¹H} NMR spectrum for **5** is assigned to the two carbonyl groups, while a broad peak at δ 69.0 in the same spectrum corresponds to the cage carbon nucleus. The ³¹P{¹H} NMR spectrum for **5** revealed a single resonance at δ 9.9, broadened due to unresolved coupling with the adjacent quadrupolar copper and boron nuclei. Spectroscopic data for compound **6** are akin to those discussed above for compound **5**: again, the symmetry of the ¹¹B{¹H} NMR spectrum indicates that the {Au(PPh₃)}⁺ fragment is fluxional with respect to the cluster surface. Physical and spectroscopic data for compounds **5** and **6** are presented in Tables 1 and 2.

Although the cationic fragments {M(PPh₃)}⁺ (M = Cu or Au) formed relatively simple bimetallic adducts upon reaction with compound **4**, it was hoped that a similar reaction using {Ir(CO)(PPh₃)₂}⁺ as the cationic transition metal synthon might produce more novel chemistry. Recent studies in our group using this iridium moiety with ferracarborane anions resulted in complexes where the iridium center either remains in an exo-polyhedral role or becomes more intimately involved in the cluster.[20]

The reaction of compound **4** with excess {Ir(CO)(PPh₃)₂}⁺, formed in situ from [IrCl(CO)(PPh₃)₂] and TlPF₆, yielded two isolatable, neutral iridium−rhenium−carborane com-

(18) (a) Jeffery, J. C.; Ruiz, M. A.; Sherwood, P.; Stone, F. G. A. *J. Chem. Soc., Dalton Trans.* **1989**, 1845. (b) Carr, N.; Gimero, M. C.; Goldberg, J. E.; Pilotti, M. U.; Stone, F. G. A.; Topaloglu, I. *J. Chem. Soc., Dalton Trans.* **1990**, 2253. (c) Jeffery, J. C.; Jelliss, P. A.; Stone, F. G. A. *J. Chem. Soc., Dalton Trans.* **1993**, 1073.

(19) (a) Kang, H. C.; Do, Y.; Knobler, C. B.; Hawthorne, M. F. *Inorg. Chem.* **1988**, *27*, 1716. (b) Park, Y.; Kim, J.; Kim, S.; Do, Y. *Chem. Lett.* **1993**, 121. (c) Adams, K.J.; Cowie, J.; Henderson, S. G. D.; McCormick, G. J.; Welch, A. J. *J. Organomet. Chem.* **1994**, *481*, C9.

(20) Franken, A.; McGrath, T. D.; Stone, F. G. A. *J. Am. Chem. Soc.* **2006**, *128*, 16169.

Chart 4

7

8
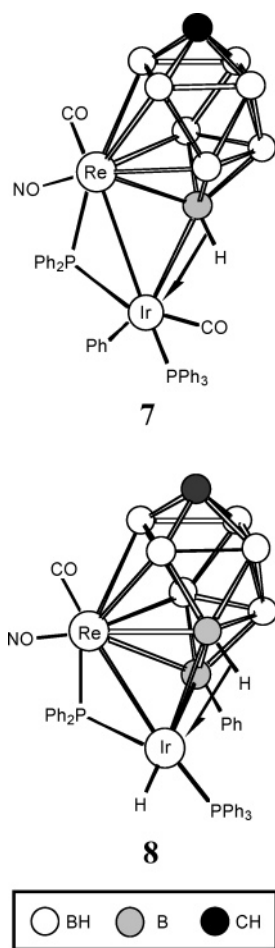
plexes, namely [6,10-{Ir(μ-PPh$_2$)(Ph)(CO)(PPh$_3$)}-10-(μ-H)-6-CO-6-NO-*closo*-6,1-ReCB$_8$H$_8$] (**7**) and [6,9,10-{Ir(μ-PPh$_2$)-(H)(PPh$_3$)}-9-(μ-H)-6-CO-6-NO-10-Ph-*closo*-6,1-ReCB$_8$H$_8$] (**8**) (see Chart 4). The relative yields of these complexes are sensitive to reaction time and the amount of {Ir(CO)(PPh$_3$)$_2$}$^+$ employed. Extended reaction times favor formation of compound **8** over compound **7**, indicating that **7** is likely to be an intermediate en route to **8**. The structures of both compound **7** and **8** were established by X-ray diffraction studies, the results of which are depicted in Figures 6 and 7, respectively. Physical and spectroscopic data were obtained for these complexes and are listed in Tables 1 and 2.

Compound **7** can be seen as a single-cluster species that retains the {*closo*-ReCB$_8$} core of its precursor **4**, with an iridium unit attached in an exo-polyhedral site. This draws some comparisons with compounds **5** and **6**. However, in compound **7** the exo-iridium is more intimately bound to the central cluster, being attached via a B–H→Ir agostic-type interaction, with Ir(61)···B(10) = 2.302(5) Å, and by a direct Re–Ir bond [Re(6)–Ir(61) = 2.8957(3) Å]. This latter connectivity is bridged by a {PPh$_2$} moiety [Ir(61)–P(661) = 2.3141(11) Å, Re(6)–P(661) = 2.4508(12) Å]. This phosphido bridge clearly originates from a PPh$_3$ ligand of the precursor {Ir(CO)(PPh$_3$)$_2$}$^+$, as the exo-polyhedral iridium unit in **7** also contains a σ-bonded Ph group [Ir(61)–C(15) = 2.117(4) Å]. The iridium center formally has a +3
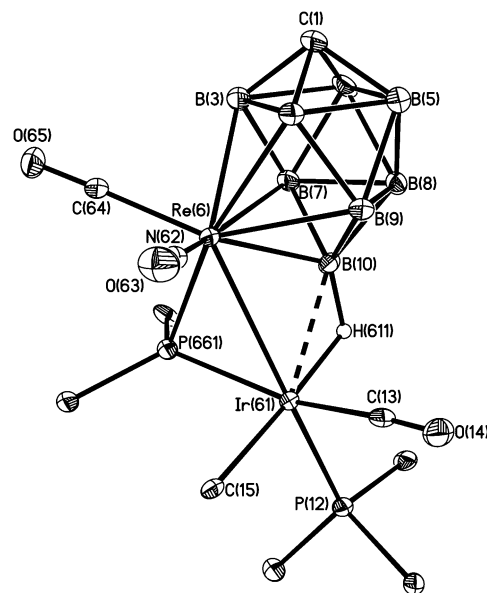
Figure 6. Structure of compound **7** showing the crystallographic labeling scheme. Only the ipso carbon atoms of the phenyl rings are shown for clarity. Selected distances (Å) are Ir(61)–Re(6) 2.8957(3), Ir(61)–P(661) 2.3141(11), Ir(61)–P(12) 2.3317(11), Ir(61)–C(13) 1.933(4), Ir(61)···B(10) 2.302(5), C(13)–O(14) 1.132(5), Re(6)–B(2) 2.406(5), Re(6)–B(3) 2.380(5), Re(6)–B(7) 2.428(5), Re(6)–B(9) 2.402(5), Re(6)–B(10) 2.153(5), Re(6)–P(661) 2.4508(12), Re(6)–C(64) 1.990(5), Re(6)–N(62) 1.796(4), C(64)–O(65) 1.138(6), N(62)–O(63) 1.192(5). Average cage B–B and C–B distances are 1.814(7) and 1.601(7) Å, respectively.
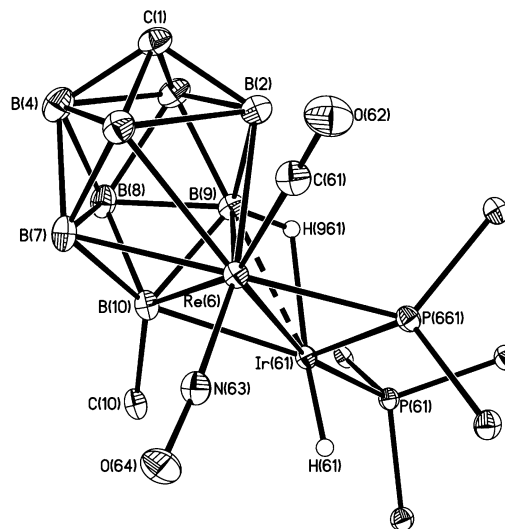
Figure 7. Structure of compound **8** showing the crystallographic labeling scheme. Only the ipso carbon atoms of the phenyl rings are shown for clarity. Selected distances (Å) are Ir(61)–Re(6) 2.8481(8), Ir(61)–P(661) 2.2272(12), Ir(61)–P(61) 2.2667(9), Ir(61)–C(10) 2.468(3), Ir(61)–B(10) 2.369(3), Ir(61)···B(9) 2.325(3), Re(6)–B(2) 2.413(3), Re(6)–B(3) 2.370(4), Re(6)–B(7) 2.443(3), Re(6)–B(9) 2.417(3), Re(6)–B(10) 2.262(3), Re(6)–P(661) 2.4177(10), Re(6)–C(61) 1.971(3), Re(6)–N(63) 1.795(3), C(61)–O(62) 1.148(6), N(62)–O(63) 1.186(3). Average cage B–B and C–B distances are 1.815(5) and 1.603(5) Å, respectively.

oxidation state and can be seen to have oxidatively inserted into a P–Ph bond of one of the phosphine ligands. Parallels can be drawn between compound **7** and [8,10-{Ir(μ-PPh$_2$)-(Ph)(CO)(PPh$_3$)}-8-(μ-H)-6,6,6,10,10-(CO)$_5$-*closo*-6,10,1-Fe$_2$CB$_7$H$_7$],[20] which also contains such a phosphido bridge derived from a PPh$_3$ ligand of {Ir(CO)(PPh$_3$)$_2$}$^+$. Such cleavage reactions for PPh$_3$ and other ligands bonded to

Table 3. Data for Crystal Structure Analyses of Compounds **1−8**

	1	**2**	**3**	**4**
formula	$C_{32}H_{29}B_8O_7PRe_2$	$C_{44}H_{39}B_8NO_7P_2Re_2$	$C_7H_{-9}B_8NO_7Re_2$	$C_{39}H_{39}B_8N_2O_3P_2Re$
fw	1015.40	1214.58	678.03	918.34
space group	$P\bar{1}$	$Pbca$	$Pna2_1$	$P2_1/c$
a, Å	9.8471(6)	16.380(3)	15.412(12)	11.3218(6)
b, Å	12.9124(8)	20.320(3)	32.481(3)	17.2378(8)
c, Å	14.4128(8)	27.594(5)	6.8793(6)	20.4936(10)
α, deg	81.938(4)	90	90	90
β, deg	88.858(3)	90	90	97.047(3)
γ, deg	80.427(3)	90	90	90
V, Å^3	1789.2(2)	9184(3)	3443.8(5)	3969.4(3)
Z	2	8	8	4
μ (Mo Kα), cm^{-1}	0.685	0.5387	1.4074	0.3183
reflns measured	67767	74382	94294	96240
indep reflns	19443	7415	11622	17300
R_{int}	0.0458	0.0913	0.0762	0.0608
wR2, R1 (all data)^a	0.0636, 0.0676	0.0638, 0.0552	0.0531, 0.0327	0.0791, 0.0542

	5	**6**	**7·CH$_2$Cl$_2$**	**8·CH$_2$Cl$_2$**
formula	$C_{21}H_{24}B_8CuNO_3PRe$	$C_{21}H_{24}B_8AuNO_3PRe$	$C_{40}H_{41}B_8Cl_2IrNO_3P_2Re$	$C_{40}H_{41}B_8Cl_2IrNO_3P_2Re$
fw	705.6	839.03	1181.46	1153.45
space group	$P\bar{1}$	$P\bar{1}$	$P\bar{1}$	$P\bar{1}$
a, Å	8.4327(9)	8.8025(9)	11.0153(14)	11.212(2)
b, Å	12.9944(13)	13.2894(14)	12.0644(15)	12.036(2)
c, Å	13.5401(14)	13.8725(14)	18.672(2)	17.608(4)
α, deg	116.193(4)	73.762(5)	103.925(6)	70.21(3)
β, deg	94.510(4)	72.345(5)	93.100(6)	77.81(3)
γ, deg	92.048(5)	88.122(5)	113.266(6)	70.50(3)
V, Å^3	1323.1(2)	1482.3(3)	2182.2(5)	2094.6(7)
Z	2	2	2	2
μ (Mo Kα), cm^{-1}	0.5459	0.9099	0.6052	0.6301
reflns measured	22623	15857	43899	40103
indep reflns	5764	7183	9833	9499
R_{int}	0.1228	0.0574	0.0489	0.0409
wR2, R1 (all data)^a	0.1001, 0.0489	0.1443, 0.0861	0.0682, 0.0362	0.0552, 0.025

^{a} wR2 = $[\Sigma\{w(F_o^2 - F_c^2)^2\}/\Sigma w(F_o^2)^2]^{1/2}$; R1 = $\Sigma||F_o| - |F_c||/\Sigma|F_o|$.

transition metal centers are long known[21] and are considered to be of significant importance in some catalytic processes.[22] This reaction system, forming **7**, is also similar to reactions of the related iridium reagent [IrMe(CO)(PR$_2$)$_2$] with [MH-(CO)$_3$(η-C$_5$H$_5$)] (M = Mo, W; R = p-tolyl,[23] Ph[24]). It has been proposed that these reactions occur between an {Ir-(CO)(PR$_3$)}$^+$ cation and an {M(CO)$_3$(η-C$_5$H$_5$)}$^-$ anion, of which the latter may be seen as quasi-isolobal[25] with the [Re(CO)$_2$(NO)(η-cage)]$^-$ anion of compound **4**. The ^{11}B-{^{1}H} NMR spectrum of **7** shows a 1:2:1:3:1 set of resonances; the peaks with multiple integrals are presumably coincidental as the complex lacks molecular symmetry. The highest frequency signal, δ 62.9, can be assigned to the Re−B(10)−Ir nucleus.[15] This resonance is particularly sharp, so that in the proton-coupled ^{11}B NMR spectrum, a small H−B coupling [J(HB) = 64 Hz] can be resolved and attributed to the B−H−Ir proton. Proton coupling could not be resolved for the other resonances, as they are significantly broader. The ^{1}H NMR spectrum for compound **7** reveals a broad resonance at δ −4.97 that also corresponds to the B−H−Ir

(21) For example: Bradford, C. W.; Nyholm, R. S. *J. Chem. Soc., Chem. Commun.* **1972**, 87.
(22) Reviews include: (a) Garrou, P. E. *Chem. Rev.* **1985**, *85*, 171. (b) van Leeuwen, P. W. N. M. *Appl. Catal., A* **2001**, *212*, 61. (c) Parkins, A. W. *Coord. Chem. Rev.* **2006**, *250*, 449.
(23) McFarland, J. M.; Churchill, M. R.; See, R. F.; Lake, C. H.; Atwood, J. D. *Organometallics* **1991**, *10*, 3530.
(24) Dahlenburg, L.; Halsch, E.; Wolski, A.; Moll, M. *J. Organomet. Chem.* **1993**, *463*, 227.
(25) Hoffman, R. *Angew. Chem., Int. Ed. Engl.* **1982**, *21*, 711.

proton. Two resonances are observed in the ^{31}P{^{1}H} spectrum at δ 106.9 (Ir−PPh$_2$−Re) and 17.2 (Ir−PPh$_3$). Unfortunately, no satisfactory ^{13}C{^{1}H} NMR spectrum could be obtained for compound **7** due to its instability in solution over the prolonged time period required for acquisition. Nevertheless, the presence of two carbonyl groups could be confirmed in its IR spectrum with strong CO absorption bands at 2060 and 2033 cm^{-1} along with an NO absorption band at 1719 cm^{-1}.

The solid-state structure of **8** shows a more condensed structure than that of **7**, as the iridium unit is now seen to cap a {B$_2$Re} triangular face. This iridium moiety is attached to the central 10-vertex {$closo$-ReCB$_8$} cluster by a B−H→Ir agostic-type interaction, with Ir(61)···B(9) = 2.325(3) Å, and by a {PPh$_2$}-bridged Re−Ir bond [Re(6)−Ir(61) = 2.8481(8) Å, Ir(61)−P(661) = 2.2272(12) Å, Re(6)−P(661) = 2.4177(10) Å], features which are similar to those present in compound **7**. In contrast to compound **7**, however, the iridium unit in **8** is also linked to the central cluster via a direct Ir−B σ-bond [Ir(61)−B(10) = 2.369(3) Å], giving a more condensed, face-capped geometry. In compound **8**, the iridium-bound carbonyl group has been lost and the Ph group that was σ-bonded to the iridium center in **7** has migrated further and is now σ-bonded to a cage boron atom [C(10)−B(10) = 1.582(4) Å]. A terminal iridium hydride completes the coordination sphere of the iridium (III) center. This Ir−H moiety is evident in the ^{1}H NMR spectrum of compound **8** with a broad resonance observed at δ −18.26; another

broader, high-field resonance (δ −4.68) in the same spectrum is assigned to the bridging B−*H*−Ir proton. The $^{11}B\{^1H\}$ NMR spectrum for **8** is also in agreement with the structure established by X-ray diffraction studies. It shows a 1:1:1:2(1 + 1 coincidence):1:1:1:1 set of resonances, further confirming the absence of molecular symmetry, of which the lowest field resonance (δ 54.8) can be assigned to the *B*−Ph nucleus as it remains a singlet in the proton-coupled ^{11}B NMR spectrum. A resonance at δ 194.8 in the $^{13}C\{^1H\}$ NMR corresponds to the single carbonyl ligand in compound **8**, and a broad peak at δ 63.4 is present due to the cage carbon atom. Similar to compound **7**, the $^{31}P\{^1H\}$ NMR spectrum for **8** shows two signals, δ 106.9 (Ir−*P*Ph$_2$−Re) and 17.2 (Ir−*P*Ph$_3$), that were assigned on the basis of their chemical shifts. The IR spectrum for **8** displays an absorption band at 2002 cm^{-1}, corresponding to the single carbonyl group present, and a peak at 1698 cm^{-1} that corresponds to the nitrosyl group.

Conclusions

The photochemical reaction of [PPh$_4$][*closo*-1-CB$_8$H$_9$] with [Re$_2$(CO)$_{10}$] to form the novel isomeric pair of dirhenacarboranes in compounds **1** and **2** demonstrates the advantage of employing photochemical synthetic techniques to form new metallacarboranes when more traditional thermal methods have failed. Compounds **1** and **2**, as well as their derivatives reported herein, constitute relatively rare examples of sub-icosahedral metal−monocarborane complexes, of which the {*closo*-10,1-ReCB$_8$} architecture in **2** is especially notable as the cage rhenium atom resides unusually in the apical site and is ligated to just four boron atoms.

Studies upon the reactivity of the anion of **1** afforded the neutral dirhenacarborane compound **3** in which, interestingly, the exo-polyhedral rhenium fragment has migrated over the surface of the central cluster and the Re−Re bond has been broken. This movement of the exo-polyhedral rhenium fragment continues in the formation of the anion of **4**, where the reaction of **3** with various donors yielded an anionic monorhenium species. Compounds **5**−**8** further illustrate how mixed-metal bimetallamonocarborane complexes can be rationally synthesized via the stepwise addition of cationic transition metal fragments to an existing anionic metallacarborane scaffold. In addition, the species **7** and **8** demonstrate a unique progression in intimacy between the {ReCB$_8$} clusters and the exo-polyhedral iridium fragment. It is anticipated that the application of similar photochemical methods for the synthesis of other metallacarboranes will lead to yet more interesting compounds and, hence, to further novel chemistry.

Experimental Section

General Considerations. Photochemical reactions were carried out in a water-cooled photolysis cell under an atmosphere of dry, oxygen-free nitrogen, using a 350 W mercury vapor arc lamp for irradiation. All other reactions were also carried out under an atmosphere of nitrogen using Schlenk line techniques. Solvents were distilled from appropriate drying agents under nitrogen prior to use. Petroleum ether refers to that fraction of boiling point 40−60 °C.

Celite pads used for filtration were typically ca. 3 cm in depth and 2 cm in diameter. Chromatography columns (ca. 20 cm in length and 2 cm in diameter) were packed with silica gel (Acros, 60−200 mesh). Preparative thin-layer chromatography (TLC) was performed on 20 × 20 cm^2 glass plates (Analtech, silica gel GF$_{254}$). NMR spectra were recorded at the following frequencies: ^{1}H, 360.13; ^{13}C, 90.56; ^{11}B, 115.5; and ^{31}P, 145.78 MHz. The compounds [PPh$_4$]-[*closo*-1-CB$_8$H$_9$],[8a] [CuCl(PPh$_3$)]$_4$,[26] [AuCl(PPh$_3$)],[27] and [IrCl(CO)-(PPh$_3$)$_2$][28] were prepared according to the literature; all other materials were used as received.

Synthesis of [PPh$_4$][6,10-{Re(CO)$_4$}-10-(μ-H)-6,6,6-(CO)$_3$-*closo*-6,1-ReCB$_8$H$_8$] (1). The reagents [PPh$_4$][*closo*-1-CB$_8$H$_9$] (0.446 g, 0.10 mmol) and [Re$_2$(CO)$_{10}$] (0.978 g, 0.15 mmol) were dissolved in THF (40 mL) in a photolysis cell and irradiated. After 2 h, volatiles were removed in vacuo, and the residue dissolved in CH$_2$Cl$_2$ (ca. 3 mL) and transferred to the top of a chromatography column. Elution with CH$_2$Cl$_2$/petroleum ether (4:1) removed an orange band, which after evaporation of solvent in vacuo, was crystallized via the slow diffusion of petroleum ether into a saturated CH$_2$Cl$_2$ solution. This gave **1** (0.517 g, 51%) as an orange crystalline solid.

Synthesis of [N(PPh$_3$)$_2$][6,10-{Re(CO)$_4$}-6-(μ-H)-10,10,10-(CO)$_3$-*closo*-10,1-ReCB$_8$H$_8$] (2). A THF (20 mL) solution of compound **1** (0.100 g, 0.01 mmol) was irradiated for 3 h (completeness monitored by ^{11}B NMR), [N(PPh$_3$)$_2$]Cl (0.058 g, 0.01 mmol) was added, and the mixture was stirred without irradiation for a further 1 h. Volatiles were then removed in vacuo, and the residue dissolved in CH$_2$Cl$_2$ (ca. 1 mL) and transferred to the top of a chromatography column. Elution with CH$_2$Cl$_2$/petroleum ether (4:1) removed a yellow band. This yellow fraction was further purified via preparative TLC using CH$_2$Cl$_2$/petroleum ether (4:1) as the liquid phase. A yellow band ($R_f = 0.55$) was removed, which after evaporation of solvent in vacuo afforded **2** (0.031 g, 26%) as a yellow powder.

Synthesis of [8,10-{Re(CO)$_4$}-8,10-(μ-H)$_2$-6,6-(CO)$_2$-6-NO-*closo*-6,1-ReCB$_8$H$_7$] (3). Compound **1** (0.200 g, 0.02 mmol) was dissolved in CH$_2$Cl$_2$ (20 mL), and NOBF$_4$ (0.010 g, 0.09 mmol) was added. After stirring at ambient temperature for 1 h, volatiles were removed in vacuo and the residue was dissolved in CH$_2$Cl$_2$ (ca. 1 mL) and transferred to the top of a chromatography column. Elution with CH$_2$Cl$_2$/petroleum ether (1:1) removed a yellow band, which after evaporation of solvent in vacuo afforded **3** (0.108 g, 81%) as a yellow powder.

Synthesis of [N(PPh$_3$)$_2$][6,6-(CO)$_2$-6-NO-*closo*-6,1-ReCB$_8$H$_9$] (4). A CH$_2$Cl$_2$ (20 mL) solution of compound **3** (0.100 g, 0.15 mmol) was treated with excess *N*,*N*,*N'*,*N'*-tetramethyldiaminomethane (0.1 mL, 0.73 mmol). After stirring at ambient temperature for 1 h, [N(PPh$_3$)$_2$]Cl (0.087 g, 0.15 mmol) was added and the mixture was stirred for a further 1 h before volatiles were removed in vacuo. The resulting residue was dissolved in CH$_2$Cl$_2$ (ca. 2 mL) and transferred to the top of a chromatography column. Elution with CH$_2$Cl$_2$ removed an orange band, which after evaporation of solvent in vacuo afforded **4** (0.098 g, 72%) as an orange microcrystalline solid.

Synthesis of [6,7,10-{Cu(PPh$_3$)}-7,10-(μ-H)$_2$-6,6-(CO)$_2$-6-NO-*closo*-6,1-ReCB$_8$H$_7$] (5). Compound **4** (0.050 g, 0.054 mmol) was dissolved in CH$_2$Cl$_2$ (10 mL), and [CuCl(PPh$_3$)]$_4$ (0.020 g, 0.014 mmol) and TlPF$_6$ (0.020 g, 0.057 mmol) were added. After stirring

(26) Jardine, F. H.; Rule, J.; Vohra, A. G. *J. Chem. Soc. A* **1970**, 238.

(27) Bruce, M. I.; Nicholson, B. K.; Bin Shawkataly, O. *Inorg. Synth.* **1989**, *26*, 325.

(28) Vrieze, K.; Collman, J. P.; Sears, C. T.; Kubota, M. *Inorg. Synth.* **1968**, *11*, 101.

at ambient temperature for 4 h, the mixture was filtered (Celite) and volatiles were removed in vacuo. The resulting residue was dissolved in CH_2Cl_2 (ca. 1 mL) and transferred to the top of a chromatography column. Elution with CH_2Cl_2/petroleum ether (1:1) removed a yellow band, which after evaporation of solvent in vacuo afforded **5** (0.029 g, 75%) as a yellow microcrystalline solid.

Synthesis of [6,7-{Au(PPh$_3$)}-7-(μ-H)-6,6-(CO)$_2$-6-NO-*closo*-6,1-ReCB$_8$H$_8$] (6). The reagents [AuCl(PPh$_3$)] (0.080 g, 0.16 mmol) and TlPF$_6$ (0.060 g, 0.17 mmol) were added to a CH_2Cl_2 (10 mL) solution of compound **4** (0.050 g, 0.054 mmol). After stirring at ambient temperature for 24 h, the mixture was filtered (Celite) and volatiles were removed in vacuo. The resulting residue was dissolved in CH_2Cl_2 (ca. 1 mL) and transferred to the top of a chromatography column. Elution with CH_2Cl_2/petroleum ether (1:1) removed a yellow band, which after evaporation of solvent in vacuo afforded **6** (0.028 g, 61%) as a yellow microcrystalline solid.

Synthesis of [6,10-{Ir(μ-PPh$_2$)(Ph)(CO)(PPh$_3$)}-10-(μ-H)-6-CO-6-NO-*closo*-6,1-ReCB$_8$H$_8$] (7) and [6,9,10-{Ir(μ-PPh$_2$)(H)-(PPh$_3$)}-9-(μ-H)-6-CO-6-NO-10-Ph-*closo*-6,1-ReCB$_8$H$_8$] (8). Compound **4** (0.075 g, 0.082 mmol) was dissolved in CH_2Cl_2 (20 mL), and [IrCl(CO)(PPh$_3$)$_2$] (0.250 g, 0.32 mmol) and TlPF$_6$ (0.110 g, 0.32 mmol) were added. After stirring at ambient temperature for 24 h, the mixture was filtered (Celite) and volatiles were removed in vacuo. The resulting residue was dissolved in CH_2Cl_2 (ca. 1 mL) and transferred to the top of a chromatography column. Elution with CH_2Cl_2/petroleum ether (1:1) removed yellow and red bands together. Further purification was achieved via preparative TLC using CH_2Cl_2/petroleum ether (1:1) as the liquid phase. A yellow band ($R_f = 0.62$) and a red band ($R_f = 0.51$) were removed, which after evaporation of solvent in vacuo gave **7** (0.018 g, 20%) and **8** (0.022 g, 25%) as yellow and red microcrystalline solids, respectively.

Structure Determinations. Experimental data for compounds **1**−**8** are listed in Table 4. Data were collected at 110(2) K on a Bruker-Nonius X8 APEX CCD area-detector diffractometer using Mo Kα radiation ($\lambda = 0.71073$ Å). Several sets of narrow data 'frames' were collected at different values of θ, for various initial values of ϕ and ω, and using 0.5° increments of ϕ or ω. The data frames were integrated using SAINT;[29] the substantial redundancy in data allowed an empirical absorption correction (SADABS)[29] to be applied, based on multiple measurements of equivalent reflections. Structures were solved by direct methods using SHELXS-97[30] and refined by full-matrix least-squares on F^2 using SHELXL-97.[31] All non-hydrogen atoms were assigned anisotropic displacement parameters. The locations of the cage carbon atoms were verified by examination of the appropriate internuclear distances and the magnitudes of their isotropic thermal displacement parameters. All hydrogen atoms in organic functions, plus terminal boron hydrogen atoms were set riding on their parent atoms in calculated positions; all other hydrogen atoms were located in difference maps and allowed positional refinement. All hydrogen atoms were assigned calculated isotropic thermal parameters [U_{iso}(H) = $1.2U_{iso}$(parent)].

Supporting Information Available: Full details of the crystal structure analyses. This material is available free of charge via the Internet at http://pubs.acs.org.

IC701496X

(29) *APEX 2*, version 2.1-0; Bruker AXS: Madison, WI, 2003.
(30) Sheldrick, G. M. *SHELXS-97*; University of Göttingen: Göttingen, Germany, 1997.
(31) Sheldrick, G. M. *SHELXL-97*; University of Göttingen: Göttingen, Germany, 1997.